Eur. Phys. J. Appl. Phys. **48**, 20501 (2009)
DOI: 10.1051/epjap/2009127

THE EUROPEAN PHYSICAL JOURNAL APPLIED PHYSICS

Regular Article

Acoustically conceal an object with hearing

B. Liu and J.P. Huang[a]

Department of Physics and Surface Physics Laboratory (National Key Laboratory), Fudan University, 220 Handan Road, Shanghai 200433, P.R. China

Received: 31 March 2009 / Received in final form: 27 April 2009 / Accepted: 6 May 2009
Published online: 3 July 2009 –

Abstract. Following the concept of remote circular electromagnetic cloaks [Phys. Rev. Lett. **102**, 093901 (2009)], here we exploit theoretically a class of rectangular cloaks that can acoustically cloak an object outside the cloaking shell. The cloaked object is no longer deafened by the cloaking shell, which is distinctly different from the existing acoustic cloaks. The function of such cloaks is justified by full wave simulations based on the finite element method. This work makes it possible to propose some applications like the stealth of submarines, which receive any incoming acoustic waves while keeping themselves undetectable to enemy's sonar devices.

PACS. 43.20.+g General linear acoustics – 43.35.+d Ultrasonics, quantum acoustics, and physical effects of sound – 43.40.+s Structural acoustics and vibration

1 Introduction

Most recently, Lai et al. [1] proposed a perfect circular invisibility cloak that can make an object outside its domain invisible. The crucial element is a complementary "antiobject" embedded inside a shell with a "folded geometry". This is different from the original perfect electromagnetic cloak [2], in which the hidden object is blind since it sits inside the cloaking shell. Lai et al.'s object is no longer blinded by the cloaking shell since it sits outside the shell. Owing to its novelty, it has soon received extensive attentions [3,4]. Apparently, if such consideration can be extended to the case of acoustics, besides enriching the realm of common acoustic scattering [5–7], more relevant applications would be desirable, such as the stealth of submarines, which may receive any incoming acoustic waves while keeping themselves undetectable to enemy's sonar devices. We noted that much work has been done, in order to achieve acoustic cloaks in the literature [8–11]. Nevertheless, all the existing acoustic cloaks make the cloaked object deafened from the incident acoustic wave because it sits inside the cloaking shell. Thus, the aim of this work is to develop the consideration of Lai et al. from electromagnetic cases to acoustic cases. For the sake of generality, we shall investigate a different shape, rectangles. The device yet to be exploited can be put in air, (pure) fluids, or suspensions as long as they can be seen as (equivalently) homogeneous acoustic media.

The remainder of this paper is organized as follows. In Section 2, we present the theoretical formalism. In Section 3, the simulation results are revealed under different conditions. This paper ends with a conclusion in Section 4.

2 Theory

Essentially, the feasibility of a two-dimensional (2D) acoustic cloak originates from the invariance property of the 2D acoustic equation in the time-harmonic form

$$\vec{\nabla}\cdot\left[\frac{1}{\rho(x,y)}\vec{\nabla}p(x,y)\right]+\frac{\omega^2}{\lambda(x,y)}p(x,y)=0, \qquad (1)$$

where $\vec{\nabla}=\frac{\partial}{\partial x}\vec{i}+\frac{\partial}{\partial y}\vec{j}$. Here $p(x,y)$ and ω are the pressure field at position (x,y) and angular frequency of an incident acoustic wave, respectively. Hence, the transformation optics method can be readily generalized to an acoustic version. Since the complementary media in the design of invisibility cloaks can be considered as a special variant of transformation media, we can also implement a similar concept in our design of acoustic cloaks. Moreover, Cummer and Schurig [8] proved that in a 2D geometry, the acoustic equations in a fluid are identical in form to the single polarization Maxwell equations via a variable exchange that also preserves boundary conditions.

As mentioned above, the genuine idea behind the ability of acoustically cloaking an external object at a specified distance outside the cloaking shell was inspired by

[a] e-mail: jphuang@fudan.edu.cn.

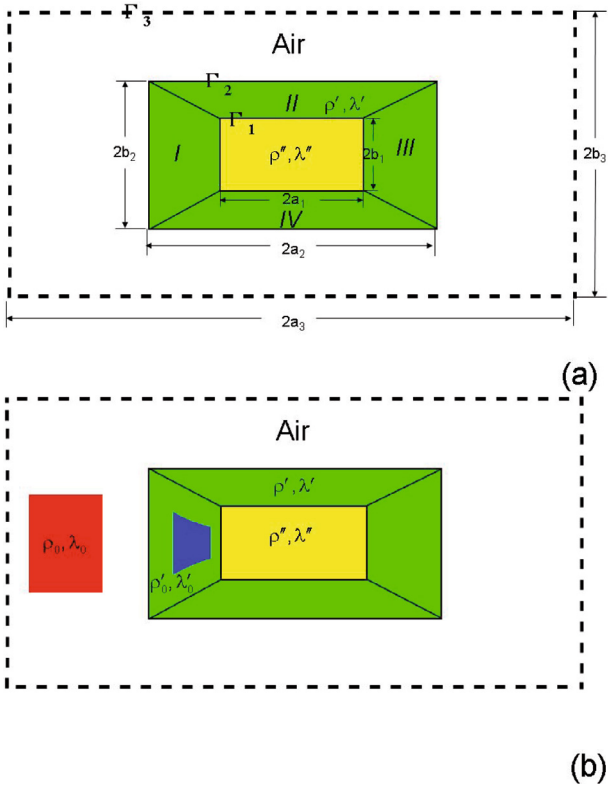

Fig. 1. (Color online) (a) Schematic graph showing a system which is composed of a rectangular shell of environmental homogeneous media like air, fluids, or suspensions (bounded by Γ_2 and Γ_3), a rectangular shell of complementary media of ρ' and λ' (bounded by Γ_1 and Γ_2) and a core material of ρ'', λ'' (within Γ_1). The system is acoustically equal to a large rectangle of the environmental homogeneous media (within Γ_3). (b) Schematically cloaking an object of ρ_0 and λ_0 by placing a complementary "image" object of ρ_0' and λ_0' in the complementary-medium shell (bounded by Γ_1 and Γ_2). In the simulations as displayed in Figures 2, 3, the environmental homogeneous media are taken to be air as a model.

Lai et al.'s work [1]. In their work, they proposed a circular invisibility cloak. And they demonstrated the effect of their design by choosing the circular case for convenience and physical clarity. In this work, besides extending their work to acoustic cases, we also consider a more complicated geometrical configuration, namely, a rectangle, to demonstrate the geometrical generality.

First, let us introduce the model for our rectangular cloak in the absence of the cloaked object, as schematically demonstrated in Figure 1a. It is worth noting that the three rectangular areas, which are respectively bounded by Γ_1, Γ_2, and Γ_3, are similar in shape, thus yielding $a_1 : a_2 : a_3 = b_1 : b_2 : b_3$. An outer shell of (environmental) homogeneous media bounded by Γ_2 and Γ_3 is canceled, from the perspective of acoustic waves, by a shell of complementary media bounded by Γ_1 and Γ_2 with general anisotropic mass density ρ' and bulk modulus λ' yet to be determined. In this work, the mass density refers to the dynamic mass density, and the bulk modulus denotes the effective bulk modulus, namely, the two material parameters that acoustic waves really experience. For the further information about the dynamic mass density and effective bulk modulus, please refer to references [12–15]. Without the loss of generality, in what follows, we choose air as a model environmental homogeneous medium, and its material parameters, namely the mass density and bulk modulus, as units. Thus, hereafter other material parameters are dimensionless quantities. The material parameters of the complementary media can be obtained by a coordinate transformation method. In detail, the surface Γ_3 is mapped to Γ_1, but the interface Γ_2 to itself. In order to achieve such a space folding, the shell should be divided into four regions (I, II, III and IV). For region I, a simple scheme of coordinate transformation between the original space (x, y, z) and transformed one (x', y', z') reads

$$x' = -\frac{a_2 - a_1}{a_3 - a_2}x - \frac{a_3 - a_1}{a_3 - a_2}a_2, \tag{2a}$$

$$y' = -\frac{a_2 - a_1}{a_3 - a_2}y - a_2\frac{a_3 - a_1}{a_3 - a_2}\frac{y}{x}, \tag{2b}$$

$$z' = z. \tag{2c}$$

Here a_1, b_1, a_2, b_2, a_3, and b_3 have been indicated in Figure 1a accordingly. Now we have the Jacobian transformation matrix between the original coordinates (x, y, z) and the transformed coordinates (x', y', z'): $\Lambda_i^{i'} = \partial x^{i'}/\partial x^i$. Here the subscript $i = x, y$, and z, and $i' = x', y'$, and z'. Similar notations hold for the following subscripts j, j', k, k', l, and l'. Cummer and Schurig gave the general transformation equations for the mass density tensor $\rho_{i'j'}$ and the bulk modulus λ' under the 2D coordinate transformation

$$\rho_{i'j'} = \det(\Lambda)^{-1}(\epsilon_{i'k'z}\Lambda_k^{k'}\epsilon_{kiz})(\epsilon_{j'l'z}\Lambda_l^{l'}\epsilon_{ljz})\rho_{ij}, \tag{3a}$$

$$\lambda' = \det(\Lambda)(\Lambda_z^{z'})^{-2}\lambda, \tag{3b}$$

where Λ is the determinant of the Jacobian matrix $\Lambda_i^{i'}$, and ϵ_{ijk} the Levi-Civita symbol. For region I, using equations (2a)–(2c), we obtain the relative mass density tensor ρ and the relative bulk modulus λ as follows

$$\rho_{x'x'} = \frac{(a_3 - a_2)^2 x'^4 + a_2^2(a_3 - a_1)^2 y'^2}{(a_3 - a_2)x'^3\Delta}, \tag{4a}$$

$$\rho_{x'y'} = \rho_{y'x'} = -\frac{a_2(a_3 - a_1)y'}{(a_3 - a_2)x'^2}, \tag{4b}$$

$$\rho_{y'y'} = \frac{\Delta}{(a_3 - a_2)x'}, \tag{4c}$$

$$\lambda' = \frac{(a_2 - a_1)^2 x'}{(a_3 - a_2)\Delta}, \tag{4d}$$

where $\Delta = (a_3 - a_1)a_2 + (a_3 - a_2)x'$. Similarly, we can obtain the material parameters in regions II, III, and IV, respectively. Specifically, parameters b_i should replace a_i in similar equations for regions II and IV. Such equations

have been purposely omitted for the compactness of this paper. Then, in order to restore the mutually canceled space bounded by Γ_1 and Γ_3 by the air shell and the complementary-medium shell, the core material is selected to have the same density as air but with a different bulk modulus a_1^2/a_3^2. Γ_1 and Γ_3 are obtained by compressing a rectangular region of air with dimensions $\{2a_3, 2b_3\}$ into a small rectangular region with $\{2a_1, 2b_1\}$, see Figure 1a. The corresponding coordinate transformation reads

$$x'' = \frac{a_1}{a_3}x, \tag{5a}$$

$$y'' = \frac{b_1}{b_3}y, \tag{5b}$$

$$z'' = z. \tag{5c}$$

When such an arrangement of core material is applied, an incident acoustic wave experiences the same traveling path as if the original rectangular region of air with dimensions $\{2a_3, 2b_3\}$ has never been changed. In this way, from the perspective of acoustic waves, the whole system, including the outer air shell, the complementary-medium shell and the core material, is equal to a rectangle of air with dimensions $\{2a_3, 2b_3\}$, and thus scatters no incident wave at all theoretically.

Second, let us consider the case of an object with relative mass density ρ_0 and relative bulk modulus λ_0 between Γ_2 and Γ_3, see Figure 1b. To cloak the object, we should include a complementary "image" object with parameters ρ_0' and λ_0'

$$\rho_{0i'j'} = \det(\Lambda)^{-1}(\epsilon_{i'k'z}\Lambda_k^{k'}\epsilon_{kiz})(\epsilon_{j'l'z}\Lambda_l^{l'}\epsilon_{ljz})\rho_{0ij}, \tag{6a}$$

$$\lambda_0' = \det(\Lambda)(\Lambda_z^{z'})^{-2}\lambda_0. \tag{6b}$$

This process is illustrated in Figure 1b. For simplicity, a rectangular object with the same horizontal symmetry axis as the cloak is placed in the left (within the shell of air between Γ_2 and Γ_3). According to equations (2a)–(2c), we can obtain the complementary "image" of the rectangular object in region I, as shown in Figure 1b. Please note the upper and the lower edges of the rectangular object with ρ_0 and λ_0 are mapped to two hyperbolic curves, respectively, rendering the shape of the "image" a curved trapezoid, due to the nonlinearity of equations (2a)–(2c). Again,we can expect that, from the perspective of acoustic waves, the object and its complementary "image" cancel each other. The whole system including the outer air shell with the cloaked object, the complementary-medium shell embedded with the complementary "image" and the core material, scatters no wave at all. Thus the effect of cloaking an external object within a specific distance outside the cloak is achieved. To verify them, we shall perform full-wave simulations based on the finite element method.

3 Simulation results

For numerical simulations, we resort to the commercial finite element simulation package COMSOL Multiphysics 3.5. First, we demonstrate the scheme shown in Figure 1a. We choose the geometric parameters $\{a_1, a_2, a_3\}$ and $\{b_1, b_2, b_3\}$ as {30, 60, 120} and {15, 30, 60} mm, respectively. Under the transformation mapping determined by equations (2a)–(2c), we obtain the parameters of the complementary media bounded by Γ_1 and Γ_2 according to equations (4a)–(4d). The corresponding ranges for the parameters of the complementary media are: $\rho_{xx} \in [-3.125, -0.5]$, $\rho_{xy} \in [-1.5, 1.5]$, $\rho_{yy} \in [-2, -0.5]$, and $\lambda \in [-0.5, -0.125]$ for region I and III, and $\rho_{xx} \in [-2, -0.5]$, $\rho_{xy} \in [-6, 6]$, $\rho_{yy} \in [-20, -0.5]$, and $\lambda \in [-0.5, -0.125]$ for regions II and IV. In all our simulations, the amplitudes of incident plane waves and cylindrical waves are 1 Pa and 100 Pa, respectively. We consider the case of an incident plane wave with frequency 10 kHz. In Figure 2a, the simulated pressure fields are shown. We can clearly identify that the cloak device itself scatters no wave. Next, we demonstrate the scheme shown in Figure 1b, namely, cloaking an external object by using complementary media. A rectangular object to be cloaked with $\rho_0 = 5$, $\lambda_0 = 1$ and dimensions {30, 40} mm, which is bounded by (–110, –80) mm horizontally and (–20, 20) mm vertically, is placed on the left of the cloak. In Figure 2b, the scattering pattern of such a single object is shown clearly. In order to achieve the effect of cloaking, we include a complementary "image" object, with material parameters obtained according to equations (6a)–(6b), into the complementary-medium shell of Figure 2a. Under this case, the ranges for the material parameters of the "image" object are: $\rho_{xx} \in [-6.25, -3.18]$, $\rho_{xy} \in [-2.25, 2.25]$, $\rho_{yy} \in [-7.86, -4.00]$, and $\lambda \in [-1.56, -0.80]$. Now the complete cloak consists of both the modified complementary-medium shell with the embedded "image" object and the core region. The simulated distribution of pressure fields is shown in Figure 2c, which definitely demonstrate the "external" cloaking effect. It should be noted that the cloaking effect does not exist in the space closely adjacent to the cloaked object since the cloaking effect originates from the embedded "image" object's canceling function. We claim that there are no geometrical or material constraints on the object to be cloaked, as long as it can be fitted into the region bounded by Γ_2 and Γ_3. Next, we show the cloaking effect of the same configuration as that in Figure 2c under a cylindrical wave with its source located at (–300, 0) mm, as shown in Figure 2d. Then we also modify the rectangular object in Figure 2b to have a mass density $\rho_0 = 1$ but a linearly changing bulk modulus of $\lambda_0 = (9 - 0.05y)/4$ (namely, λ_0 changes from 2 to 2.5 in the y direction). The material parameters of the complementary "image" object are changed according to equations (6a)–(6b). The cloaking effect of such design can be again justified, regardless of the variance of the material parameters of the cloaked object and the direction of incident plane or cylindrical waves. Such figures are not shown herein.

Then a more numerically challenging example is presented to confirm our design. Consider an object of $\rho_0 = 5$ and $\lambda_0 = 1$ existing in the form of a rectangular shell with inner dimensions {160, 80} mm and outer dimensions {200, 100} mm. Figure 3a shows its scattering pattern

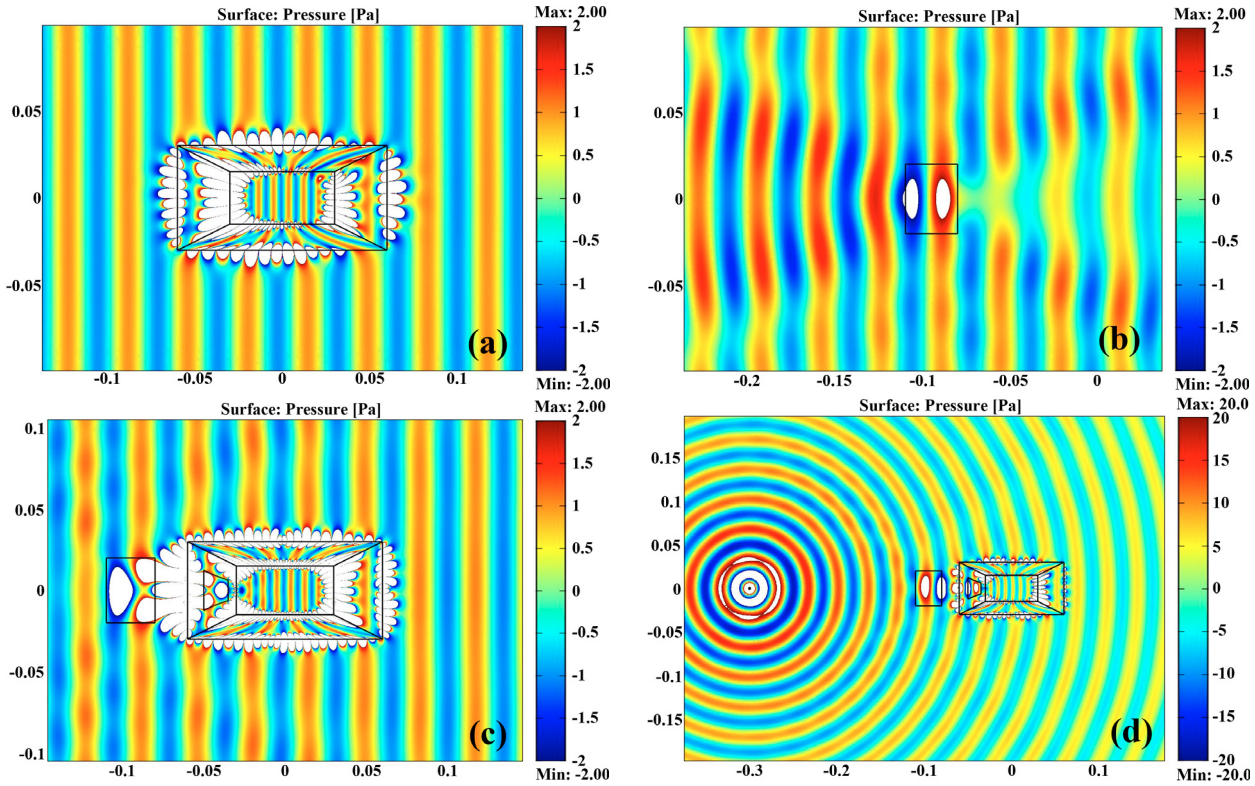

Fig. 2. (Color online) Snapshots of the distribution of pressure fields under (a)–(c) an incident acoustic plane wave and (d) a cylindrical wave with its source located at (–300, 0) mm, at frequency 10 kHz. (a) A rectangular complementary-medium shell of inner size {60, 30} mm and outer size {120, 60} mm, and a core of size {60, 30} mm. (b) A rectangular object with $\rho_0 = 5$, $\lambda = 1$, and size {30, 40} mm. (c) The rectangular object in (b) is cloaked by an acoustic cloak composed of both a rectangular shell of complementary media with an embedded curved trapezoidal "image" object and a core material. (d) shows the same geometrical and material configurations as those of (c). Note that for Figures 2, 3 meters are used as the units for both x and y axes.

under an incident plane wave with frequency 5 kHz. In this case, the "image" object is also a rectangular shell with inner dimensions {80, 40} mm and outer dimensions {100, 50} mm inside the complementary-medium shell. In Figure 3b, we show the simulated pressure-field distribution when the object is "cloaked" by a shell composed of a complementary medium with the "image" shell located inside and a core material. It should be noted that the cloaked object (shell) is outside the cloak. Apparently, the figure clearly demonstrates the cloaking effect. The same cloaking effect can be found in Figures 3c–3f, where we investigate an cylindrical acoustic wave with both quasi-normal and oblique incidence.

4 Discussion and conclusion

Here some comments are in order. We have observed the definite convergence to the perfect cloaking effect (which corresponds to some necessary conditions, e.g., zero reflection and/or full transmission) when the finite element mesh gets finer and finer. In other words, the reflection coefficient, if it is non-zero in the presence of a cloak, is solely due to the numerical error arising in the simulations with specific meshes. On the other hand, we have demonstrated that the finite element method in use yields more accurate results (namely, better cloaking effects) under the same mesh when the frequency is decreased. Thus, in the simulations with given meshes, lower frequencies pose less challenge to achieve perfect cloaking. However, for a high frequency, much more computational time should be consumed because for achieving perfect cloaking the mesh must be refined sufficiently. In this work, the two frequencies, 5 or 10 kHz, are only selected as a model, in order to display the effects of both scattering and cloaking. In this sense, the present quality of Figures 2 and 3 is actually the outcome of the compromise between simulation accuracy and computational time.

As mentioned above, the cloaking effect does not exist in the space closely adjacent to the cloaked object. This has nothing to do with the near/far field limit since it is an intrinsic characteristic of our design, regardless of the kind of wave sources. Our design can only guarantee the cloaking effect outside the boundary Γ_3, because the cloaking effect originates from the canceling effect between the homogeneous media shell and the complementary media shell. Inside Γ_3, the canceling process can result in highly fluctuating pressure distribution, which just explains why there exist the regions where the value of the

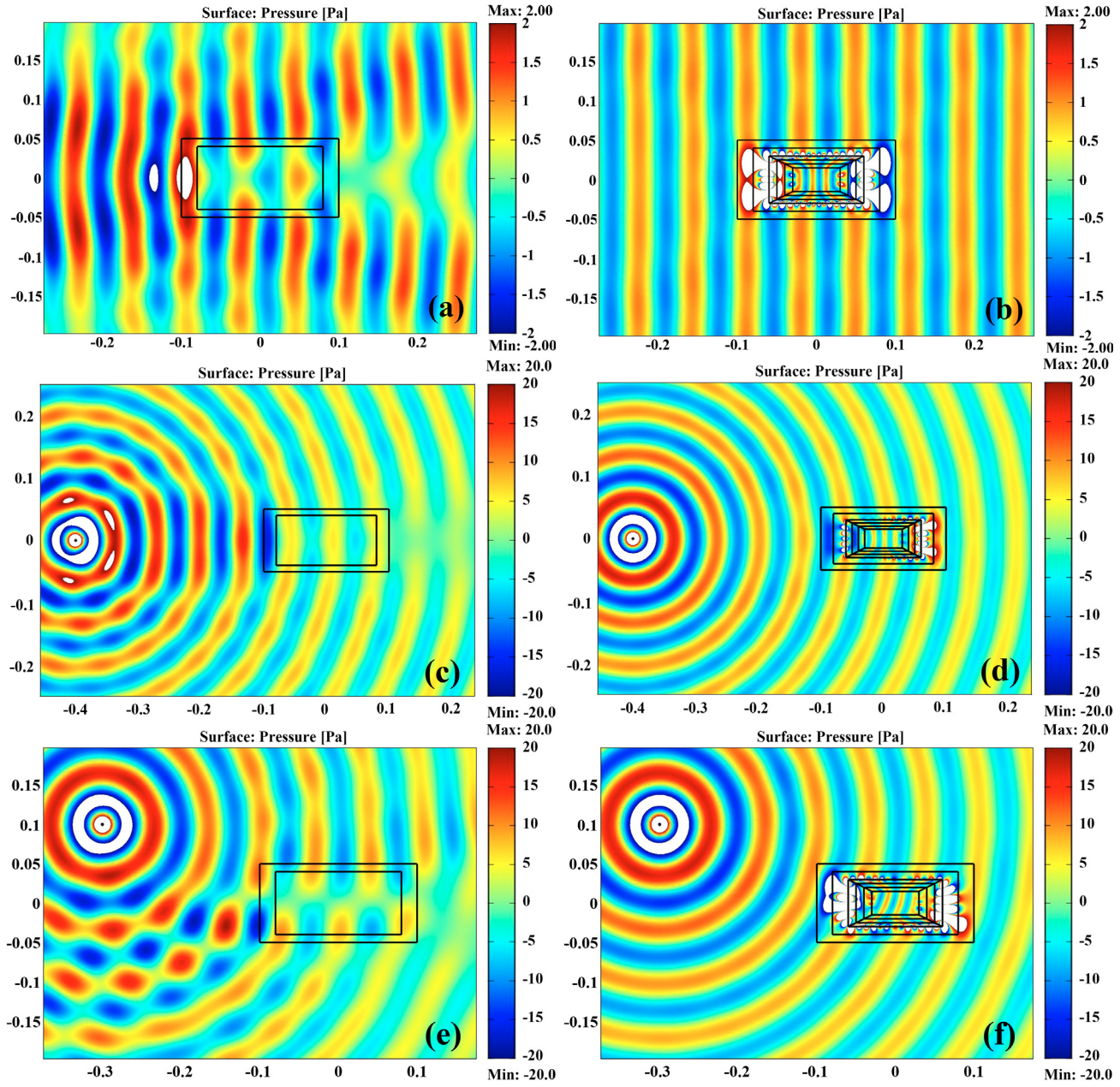

Fig. 3. (Color online) Snapshots of the distribution of pressure fields under (a)–(b) an incident acoustic plane wave, (c)–(d) a cylindrical wave with its source located at (–400, 0) mm, and (e)–(f) a cylindrical wave with its source located at (–300, 100) mm, at frequency 5 kHz. (a, c, e): a rectangular shell of $\rho_0 = 5$ and $\lambda_0 = 1$. (b, d, f): the rectangular shell of (a), (c), or (e) is cloaked by an acoustic cloak composed of both a rectangular shell of complementary media with an embedded "image" shell and a core material.

amplitude of pressure fields exceeds the bounds of bars (as displayed in white in Figs. 2 and 3).

In fact, the choice of air instead of water as "(environmental) homogeneous media bounded by Γ_2 and Γ_3" made no qualitative change in the underlying physics of our work. Since essentially we chose the material parameters of the (environmental) homogeneous media as units, switching between air and water does not change any formulae. The only difference exists in the process of simulations, where the material parameters of the (environmental) homogeneous media are altered from air to water. Apparently, the quantitative simulated results will change, but we can readily "renormalize" the color bars to obtain the same pattern of pressure distribution. In this sense, as already mentioned above, the device can be put in air, (pure) fluids, or suspensions as long as they can be seen as (equivalently) homogeneous acoustic media.

In summary, inspired by reference [1], we have proposed a design of rectangular acoustic cloaks that can conceal an object outside its domain. They are distinctly

different from the existing acoustic cloaks because the hidden object in the present cloaks is no longer deafened. In principle, the special materials required for our design can be achieved using local resonances [12–15].

We are very grateful to Dr. J.J. Xiao for his fruitful discussion, Prof. S.A. Cummer for his helpful advice, and Ms. Y.F. Pan for her assistance in plotting the figures. Also, we acknowledge the financial support by the National Natural Science Foundation of China under Grant Nos. 10604014 and 10874025, and by Chinese National Key Basic Research Special Fund under Grant No. 2006CB921706.

References

1. Y. Lai, H. Chen, Z.-Q. Zhang, C.T. Chan, Phys. Rev. Lett. **102**, 093901 (2009)
2. J.B. Pendry, D. Schurig, D.R. Smith, Science **312**, 1780 (2006)
3. A. Cho, Science **323**, 701 (2009)
4. T. Philbin, Physics **2**, 17 (2009)
5. K. Kwon, B.G. Loh, D.R. Lee, Eur. Phys. J. Appl. Phys. **40**, 343 (2007)
6. I. Nunez, A. Arzua, T.D. Campos, Eur. Phys. J. Appl. Phys. **42**, 169 (2008)
7. A. Duclos, D. Lafarge, V. Pagneux, Eur. Phys. J. Appl. Phys. **45**, 11302 (2009)
8. S.A. Cummer, D. Schurig, New J. Phys. **9**, 45 (2007)
9. H. Chen, C.T. Chan, Appl. Phys. Lett. **91**, 183518 (2007)
10. S.A. Cummer, B.I. Popa, D. Schurig, D.R. Smith, J.B. Pendry, M. Rahm, A. Starr, Phys. Rev. Lett. **100**, 024301 (2008)
11. Y. Cheng, X.J. Liu, J. Appl. Phys. **104**, 104911 (2008)
12. J. Li, C.T. Chan, Phys. Rev. E **70**, 055602 (2004)
13. J. Mei, Z. Liu, W. Wen, P. Sheng, Phys. Rev. Lett. **96**, 024301 (2006)
14. P. Sheng, J. Mei, Z. Liu, W. Wen, Physica B **394**, 256 (2007)
15. Z. Yang, J. Mei, M. Yang, N.H. Chan, P. Sheng, Phys. Rev. Lett. **101**, 204301 (2008)